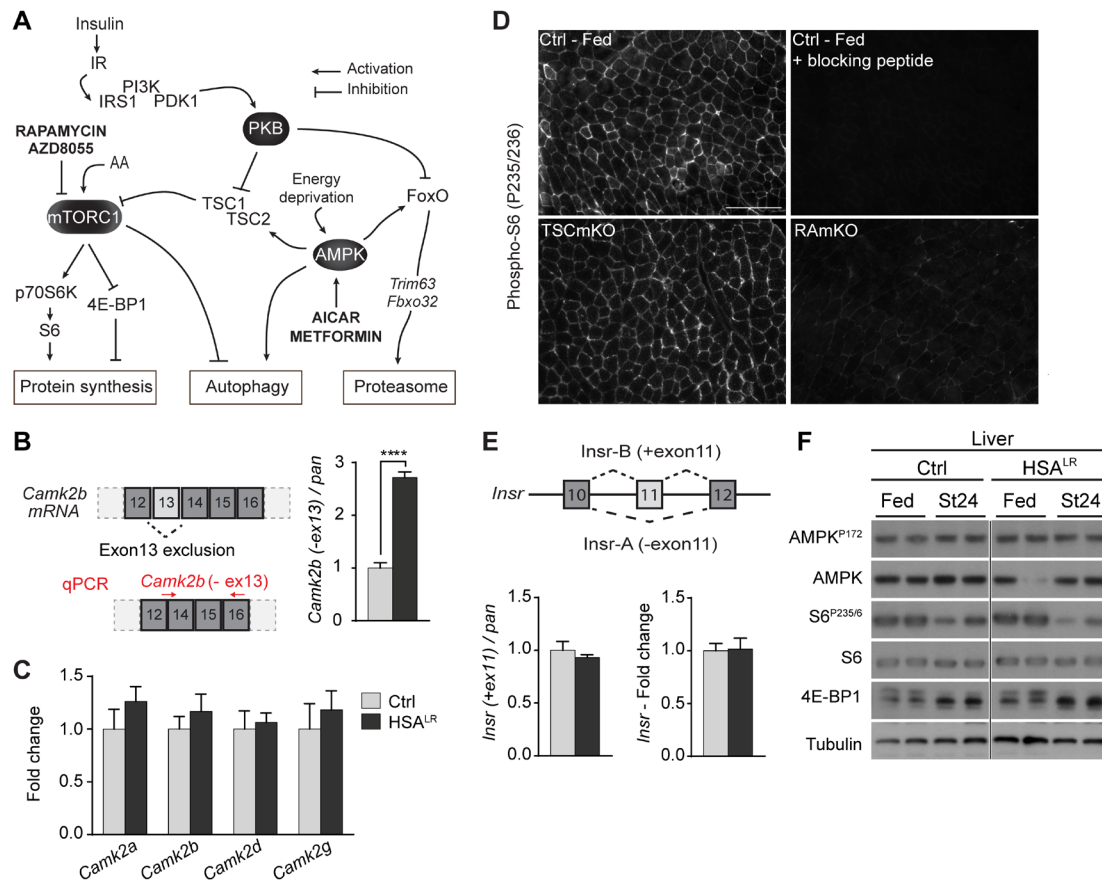


Supplemental Material

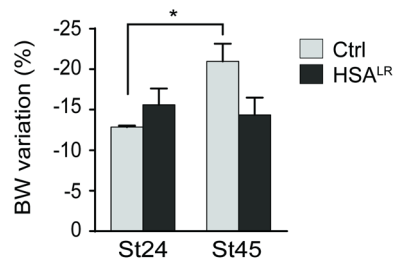
Targeting deregulated AMPK and mTORC1 pathways improves muscle function in myotonic dystrophy type I

Marielle Brockhoff, Nathalie Rion, Kathrin Chojnowska, Tatiana Wiktorowicz, Christopher Eickhorst, Beat Erne, Stephan Frank, Corrado Angelini, Denis Furling, Markus A. Rüegg, Michael Sinnreich and Perrine Castets

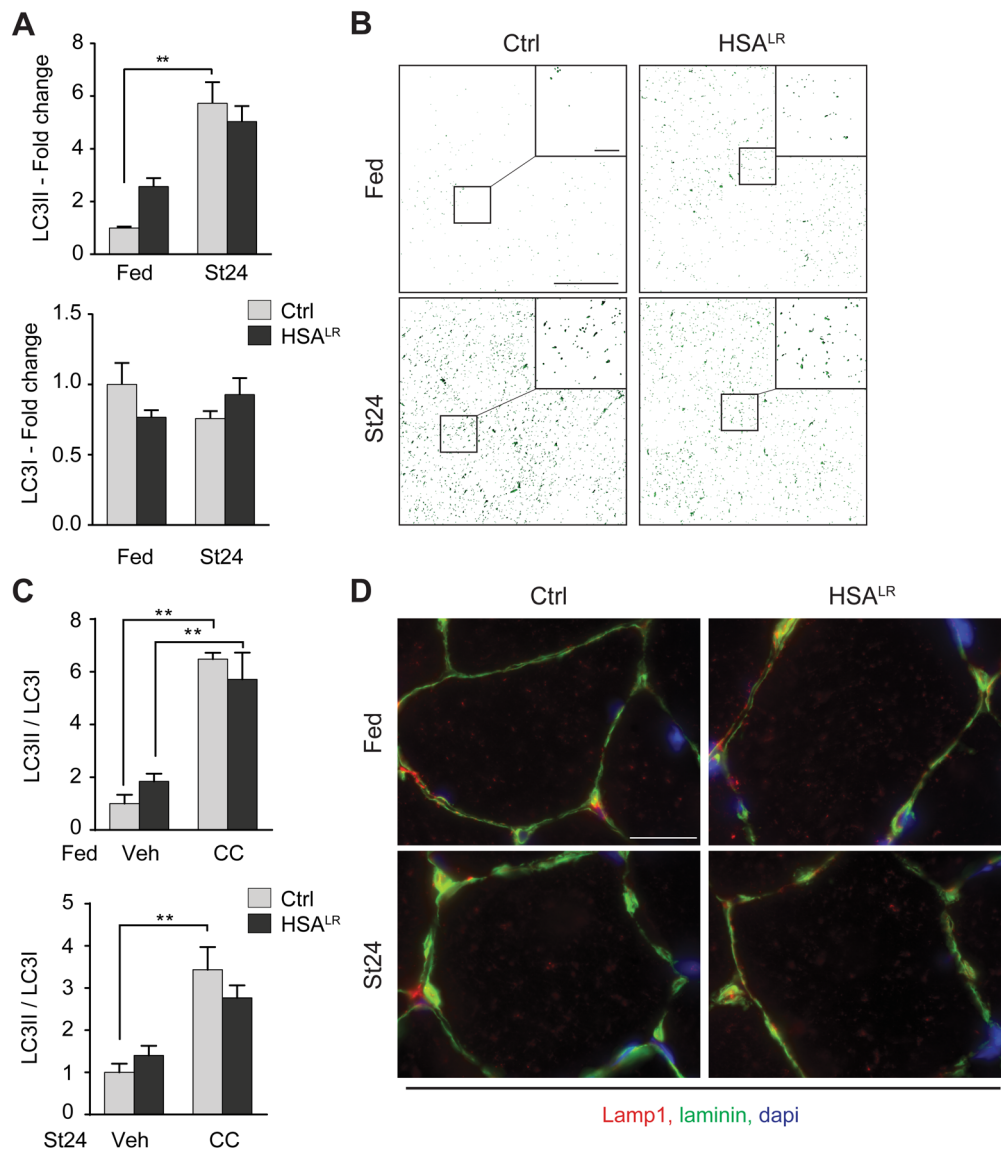
Supplemental material includes: 7 supplemental figures, 2 supplemental tables and supplemental methods



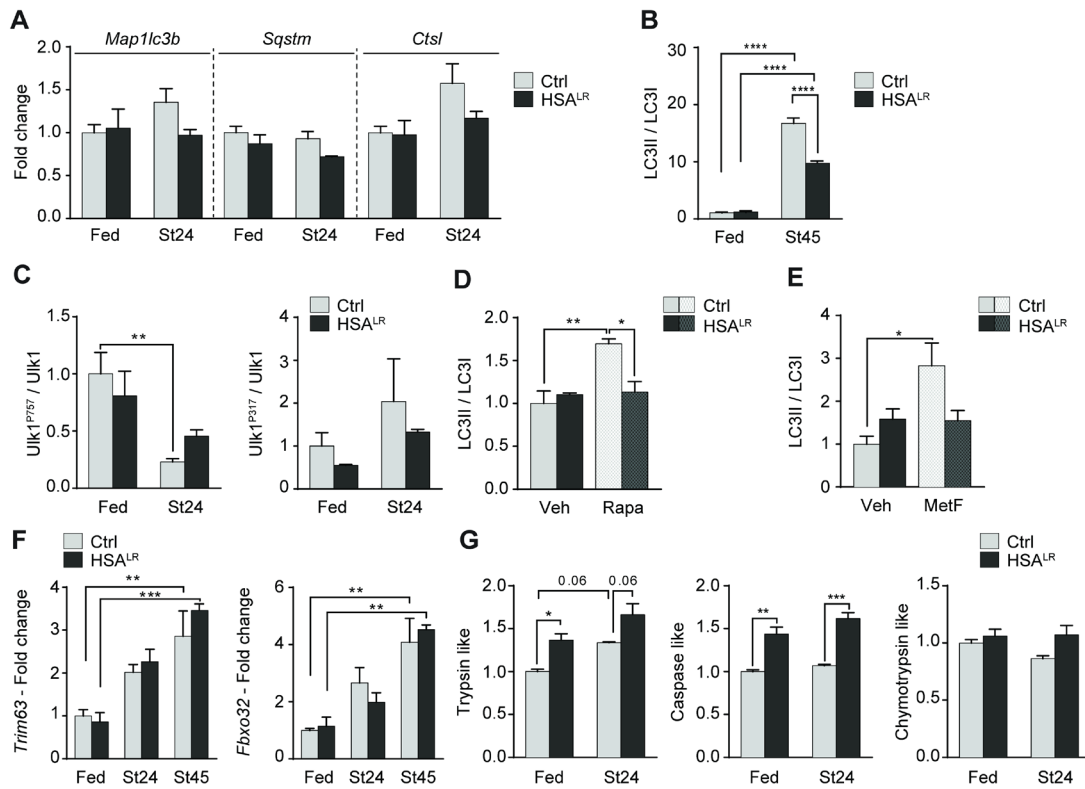
Supplemental Figure 1. Imbalance in AMPK / mTORC1 pathways is not related to insulin receptor (IR)-PKB/Akt deregulation and is limited to muscle tissue in HSA^{LR} mice. (A) Simplified scheme of the metabolic signaling involved in proteostasis in skeletal muscle. (B) Representation of the known alternative splicing of *Camk2b* mRNA in DM1 (exon 13 exclusion) and of the primers used to quantify its expression. Quantitative PCR shows increased levels of *Camk2b* transcript with exon 13 exclusion (-ex13) in HSA^{LR} muscle. n=4 per group. (C) Transcript levels of *Camk2a*, *2b*, *2d* and *2g* are not affected in HSA^{LR} muscle (n=4). Expression is normalized to *Actn*. (D) Immunostaining shows the expected depletion and accumulation of phospho-S6 in RAmKO (mTORC1 inhibition) and TSCmKO (mTORC1 activation) muscles, respectively. Immunostaining in the presence of the S6^{P235/6} blocking peptide further confirms the specificity of the staining. Scale bar, 200 μ m. (E) Splicing of the *Insr* gene, corresponding to the mis-splicing event in DM1 patients, is not altered in muscle from 2 month-old HSA^{LR} mice (n=4). (F) Imbalance in AMPK and mTORC1 signaling is not observed in liver from fed and starved (St24) HSA^{LR} mice compared to control (Ctrl) animals. The lanes were run on the same gel but were noncontiguous. Data are relative to control (B, C and E) and represent mean \pm SEM. ****p<0.0001, unpaired two tailed Student's t-test (B).



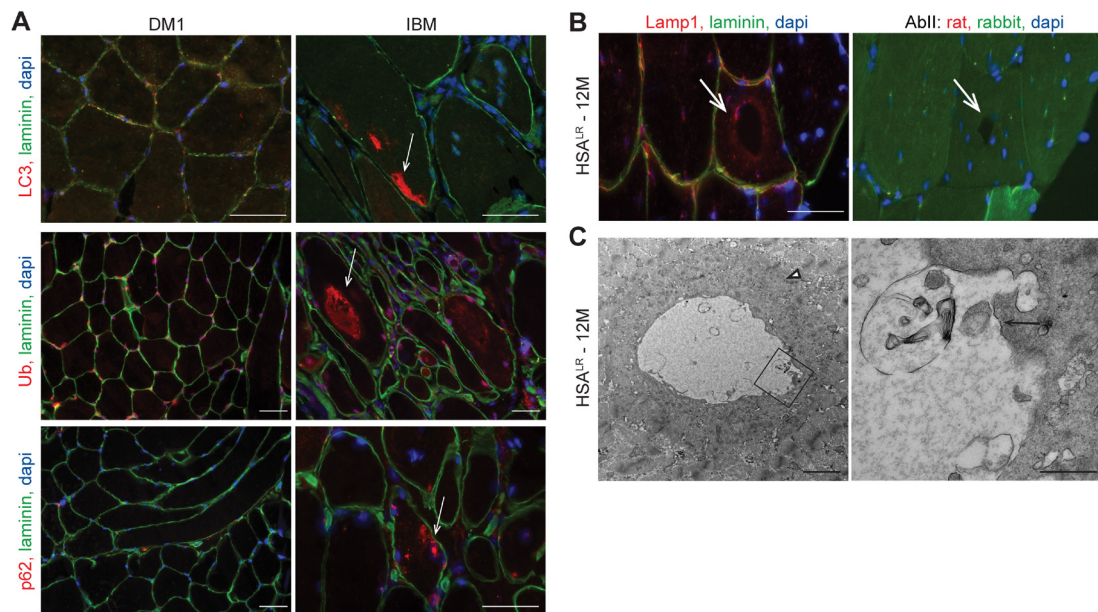
Supplemental Figure 2. HSA^{LR} mice display resistance to prolonged starvation. Loss of body weight increases from 24 to 45 h of starvation in control (Ctrl) mice but not in HSA^{LR} mice. Loss is expressed as a percentage of the initial body weight. n=4 Ctrl and 3 HSA^{LR}. *p<0.05, 2-way ANOVA with Tukey's multiple comparisons test correction.



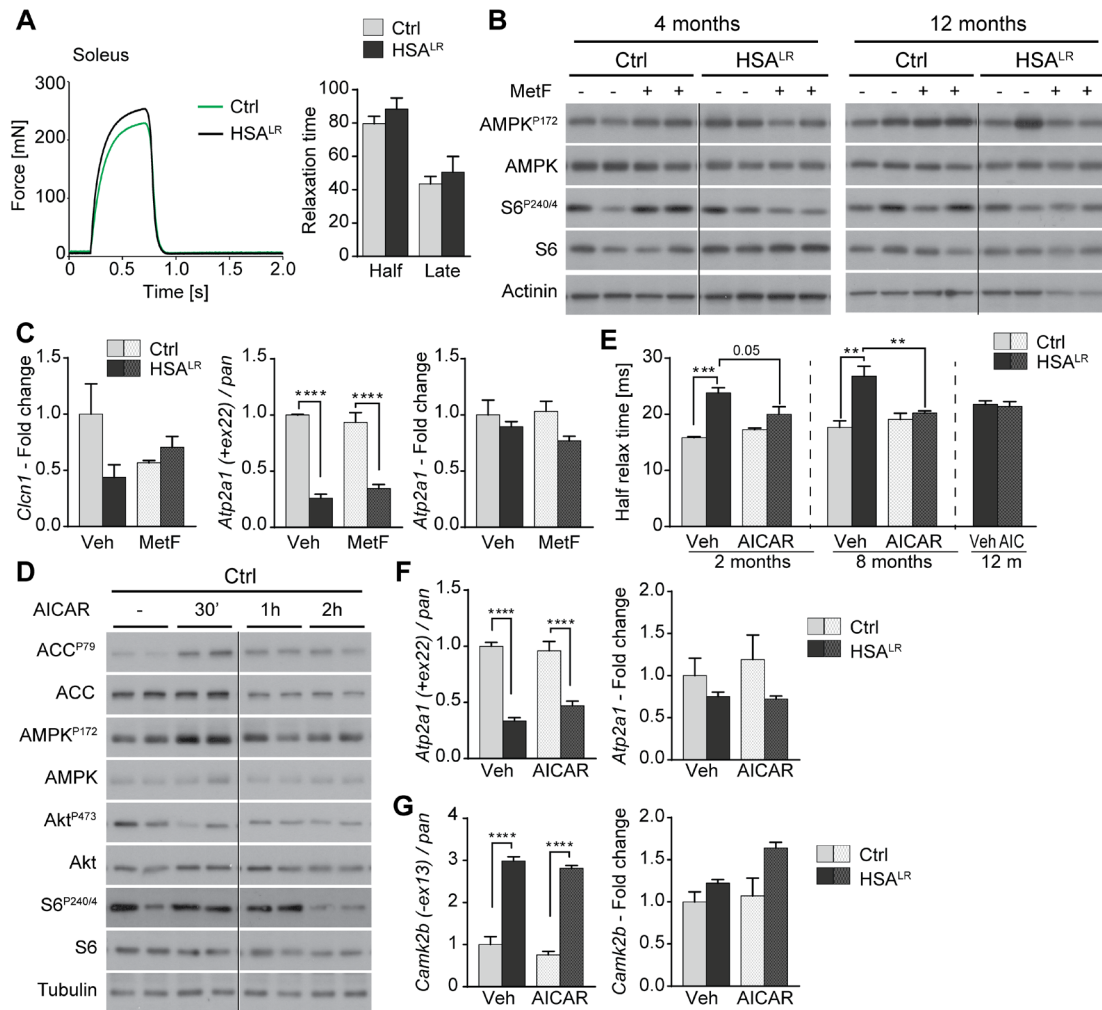
Supplemental Figure 3. HSA^{LR} muscles display perturbed autophagic flux. (A) Quantification of immunoblots for LC3II and LC3I in TA muscle from fed and starved (St24) control (Ctrl) and HSA^{LR} mice. Protein expression is normalized to α -actinin (A, n=3 fed and 7/6 starved Ctrl/HSA^{LR}). (B) Digital image after thresholding displays GFP-LC3 puncta in muscle fibers analyzed by confocal microscopy (see Figure 3B). Scale bar, 50 μ m; 10 μ m for insets. (C) Quantification of the LC3II/LC3I ratio in TA muscle from fed and starved (St24) control (Ctrl) and HSA^{LR} mice, upon treatment with colchicine (CC). Fed, n=3 Ctrl and 4 HSA^{LR}; St24, n=4 Ctrl and 3 HSA^{LR}. (D) Immunostaining for Lamp1 protein (red) reveals similar lysosomal distribution in muscle from fed and starved (St24) HSA^{LR} and control (Ctrl) mice. Scale bar, 20 μ m. Data are relative to fed (A) or vehicle-treated (C) control mice. Values represent mean \pm SEM. **p<0.01, 2-way ANOVA with Tukey's multiple comparisons test correction.



Supplemental Figure 4. HSA^{LR} muscle display mild deregulation of the autophagic flux and increased proteasome activity. (A) Expression of autophagy-related genes remains unchanged in control (Ctrl) and HSA^{LR} muscle after 24 h of starvation (St24). Fed, n=4; St24, n=4 Ctrl and 3 HSA^{LR}. (B) After 45 h of starvation (St45), change in LC3II to LC3I ratio is reduced in muscle from HSA^{LR} mice (n=4 Ctrl and 3 HSA^{LR}). (C) Quantification of immunoblots for phosphorylated forms of Ulk1 in TA muscle from fed and starved (St24) control (Ctrl) and HSA^{LR} mice. Protein expression is normalized to total Ulk1. n=3 fed and 4 starved per genotype. (D, E) After rapamycin (Rapa - D) or metformin (MetF - E) treatment, LC3II/LC3I ratio is increased in control muscle but not in HSA^{LR} muscle. Veh (D), n=4 Ctrl and 3 HSA^{LR}; Rapa, n=3; Veh (E), n=3; MetF, n=4 per genotype. (F) Expression of atrogenes is efficiently induced in HSA^{LR} muscle upon 45 h of starvation (St45). Expression is normalized to *Actn* (n=4 Ctrl and 4/3 fed/starved HSA^{LR}). (G) Trypsin- and caspase-like activities are increased in muscle from fed and starved (St24) HSA^{LR} mice, compared to control (Ctrl) mice in the same nutritive condition (n=3). Data are relative to control mice in fed conditions (A, B, C, F, G) or to vehicle-treated control mice (D, E). Values represent mean \pm SEM. *p<0.05, **p<0.01, ***p<0.001, ****p<0.0001, 2-way ANOVA with Tukey's multiple comparisons test correction.

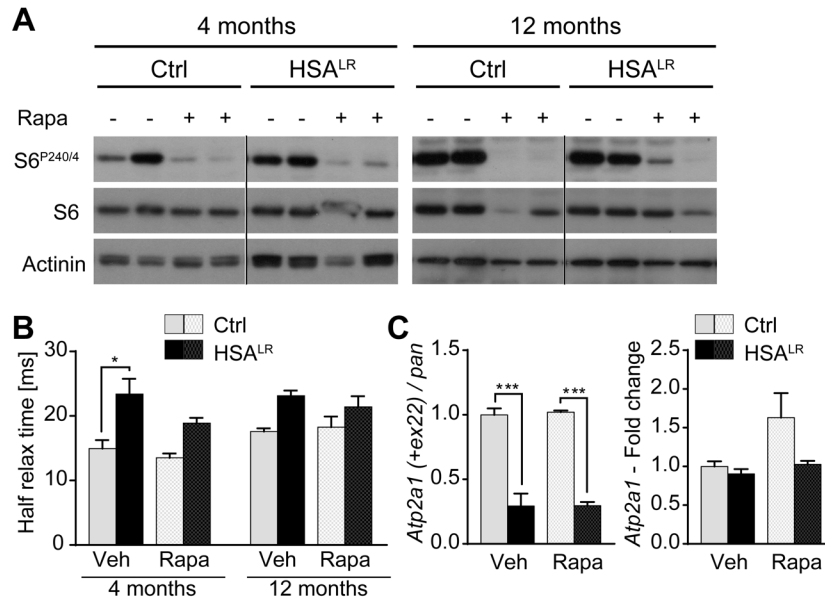


Supplemental Figure 5. Few autophagic features are observed in muscle from DM1 patients and HSA^{LR} mice. (A) Muscle biopsies from DM1 patients display no accumulation of LC3 (red, upper panel), ubiquitinated proteins (red, middle panel) or p62 (red, lower panel) by immunostaining, contrasting with muscle from an IBM patient (arrow). Scale bar, 50 μ m. (B) Immunostaining on serial muscle sections from 12-month (M)-old HSA^{LR} mice shows high density of lysosomes, reacting with anti-Lamp1 antibodies (red), at the periphery of a vacuole; no positive staining is observed in the negative control with only secondary antibodies (red, anti-rat) in the region of the same vacuole. Scale bar, 50 μ m. (C) Electron microscopy confirms the presence of vacuolar structures in muscle from 12-month (M)-old HSA^{LR} mice. Vacuoles are limited by discontinuous membrane structures (arrow) and surrounded by disorganized regions of contractile materials (arrowhead). Scale bar, 2 μ m for left panel; 0.5 μ m for right panel.



Supplemental Figure 6. AICAR and metformin treatments have distinct effects on DM1 muscle function and splicing. (A) In vitro tetanic stimulation (120 Hz) of the *soleus* muscle leads to contraction of HSA^{LR} and control muscles; half and late relaxation times are not increased in mutant *soleus* muscle. (B) A ten-day oral treatment with metformin does not lead to reproducible decreased S6 phosphorylation in control (Ctrl) and mutant muscles. Samples were run on the same gel but were noncontiguous. (C) The overall expression of the *Cln1* gene, as well as splicing and transcript expression of the *Atp2a1* gene are not changed in muscle from metformin (MetF)-treated HSA^{LR} mice, compared to vehicle (Veh)-treated mutant mice (n=3 per group). (D) Immunoblots for phospho- and total ACC, AMPK, PKB/Akt and S6 proteins show efficient phosphorylation of AMPK and ACC, 30 min after AICAR injection in control (Ctrl) muscle. Phosphorylation of S6, an AMPK-indirect target, is strongly reduced 2 h after AICAR injection, while no major change in PKB/Akt activity is detected. (E) Half relaxation time is reduced in muscle from 2- (n=3 Ctrl and 4 HSA^{LR}) and 8- (n=3 Ctrl and 6/7 Veh/AICAR HSA^{LR}) month-old HSA^{LR} mice treated with AICAR, as compared with untreated (Veh) mutant mice. n=4/5 12-month-old Veh/AICAR HSA^{LR}. (F, G) Mis-splicing and transcript expression of *Atp2a1* (F, n=3 Ctrl and 5 HSA^{LR}) and *Camk2b* (G, n=3 per group) genes are not changed in muscle from AICAR-treated HSA^{LR} mice, compared to vehicle (Veh)-treated mutant

mice. Values represent mean \pm SEM. ** $p < 0.01$, *** $p < 0.001$, **** $p < 0.0001$, 2-way ANOVA with Tukey's multiple comparisons test correction.



Supplemental Figure 7. Rapamycin treatment efficiently inhibits mTORC1 signaling but impacts neither on half relaxation time nor on splicing. (A) Immunoblots for phospho- and total S6 proteins reveal efficient mTORC1 inhibition in 4- and 12-month-old, rapamycin (Rapa)-treated control (Ctrl) and HSA^{LR} mice. (B) Half relaxation time remains unchanged upon rapamycin (Rapa) treatment of HSA^{LR} mice, as compared to vehicle (Veh)-treated mutant mice (n=4 Ctrl and 8/10 Veh/Rapa HSA^{LR} at 4 months of age; n=3 Ctrl and 5/6 Veh/Rapa HSA^{LR} at 12 months of age). (C) Rapamycin treatment does not change splicing and expression of the *Atp2a1* gene in mutant mice (n=3 Ctrl and 4 HSA^{LR}). Values represent mean \pm SEM. *p<0.05, ***p<0.001, 2-way ANOVA with Tukey's multiple comparisons test correction.

Supplemental Table 1. Changes in EDL muscle mass and twitch forces upon treatments in HSA^{LR} and control mice

	Ctrl		HSA ^{LR}	
	Vehicle	AICAR	Vehicle	AICAR
EDL mass/BW (‰)				
2M	0.44 ± 0.01	0.42 ± 0.01	0.51 ± 0.03 [#]	0.48 ± 0.01
8M	0.40 ± 0.02	0.42 ± 0.03	0.45 ± 0.03	0.36 ± 0.02
12M	-	-	0.40 ± 0.01	0.38 ± 0.02
Pt (mN)				
2M	15.40 ± 1.45	22.04 ± 0.84 ^{**}	12.22 ± 0.50	25.14 ± 1.16 ^{***}
8M	30.68 ± 5.08	29.93 ± 3.21	24.02 ± 1.35	25.85 ± 1.51
12M	-	-	29.27 ± 2.86	37.50 ± 1.48 ^{0.06}
sPt (mN/mm ²)				
2M	11.18 ± 0.92	16.84 ± 1.03 ^{**}	10.51 ± 0.60	15.58 ± 0.72 ^{**}
8M	20.16 ± 3.33	18.06 ± 2.52	13.08 ± 1.02 [#]	15.24 ± 0.86
12M	-	-	12.01 ± 1.39	16.18 ± 0.64 [*]
	Vehicle	Rapamycin	Vehicle	Rapamycin
EDL mass/BW (‰)				
4M	0.38 ± 0.02	0.37 ± 0.02	0.42 ± 0.02	0.43 ± 0.01
12M	0.36 ± 0.03	0.33 ± 0.02	0.38 ± 0.02	0.32 ± 0.03
Pt (mN)				
4M	20.58 ± 1.69	17.77 ± 0.80	19.61 ± 1.55	29.70 ± 2.23 ^{***#}
12M	22.40 ± 4.12	19.17 ± 0.35	17.69 ± 3.92	20.51 ± 2.18
sPt (mN/mm ²)				
4M	12.50 ± 1.71	11.08 ± 0.54	9.71 ± 0.89	15.23 ± 1.18 ^{**}
12M	13.72 ± 3.08	13.93 ± 1.25	9.26 ± 1.97	11.77 ± 1.46
	Vehicle	AZD8055	Vehicle	AZD8055
EDL mass/BW (‰)	0.37 ± 0.02	0.34 ± 0.02	0.42 ± 0.02	0.41 ± 0.01
Pt (mN)	32.01 ± 3.43	31.53 ± 0.54	26.58 ± 2.68	35.55 ± 0.64 ^{**}
sPt (mN/mm ²)	19.85 ± 3.42	18.84 ± 0.07	10.60 ± 2.31 [#]	17.32 ± 0.44 [*]

BW, body weight; Pt, twitch force. AICAR, 2-month-old (n=3 Ctrl and 4 HSA^{LR}), 8-month-old (n=3 Ctrl and 6/7 Veh/AICAR HSA^{LR}), 12-month-old (n=4/5 Veh/AICAR HSA^{LR}) mice; Rapamycin, 4-month-old (n=4 Ctrl and 8/10 Veh/Rapa HSA^{LR}), 12-month-old (n=3 Ctrl and 5/6 Veh/Rapa HSA^{LR}) mice; AZD8055 (8-month-old, n=3 Ctrl and 5/8 Veh/AZD HSA^{LR}). Values are mean ± SEM. # p< 0.05, ## p<0.01 compared to control mice with same treatment; * p<0.05, ** p<0.01, *** p<0.001 compared to same genotype treated with vehicle, 2-way ANOVA with Tukey's multiple comparisons test correction – For 12-month-old AICAR-treated mice: * p<0.05 compared to same genotype treated with vehicle, unpaired two tailed Student's t-test. *M*: month.

Supplemental Table 2. List of primers

Gene	Forward primer	Reverse primer
<i>ACTA1 (human)</i>	5'-CGAGACCACCTACAACAGCA-3'	5'-GGCATACAGGTCCTTCCTGA-3'
<i>Acta1 (mouse)</i>	5'-CCGGAAAGAAATCTCAACCA-3'	5'-CCAAGTCCTGCAAGTGAACA-3'
<i>Actn</i>	5'-CTGGTCTTCGACAACAAGCA-3'	5'-TTGTCAGGATCTGGGTCTCC-3'
<i>Atp2a1 +ex22</i>	5'-GCCCTGGACTTTACCCAGTG-3'	5'-ACGGTTCAAAGACATGGAGGA-3'
<i>Atp2a1 pan</i>	5'-GCCCTGGACTTTACCCAGTG-3'	5'-CCTCCAGATAGTTCCGAGCA-3'
<i>Camk2a</i>	5'-TTTGCCCTCTCAGGCTTTA-3'	5'-GTGGACAGGGGCATGTTAG-3'
<i>Camk2b -ex13</i>	5'-TTTCTCAGCAGCCAAGAGTTT-3'	5'-TTCCTTAATCCCGTCCACTG-3'
<i>Camk2b pan</i>	5'-GCACGTCATTGGCGAGGAT-3'	5'-ACGGGTCTCTTCGGACTGG-3'
<i>Camk2d</i>	5'-CTGGCACACCTGGGTATCTT-3'	5'-ATCCAGAAGGGTGGGTATC-3'
<i>Camk2g</i>	5'-ACCGACGACTACCAGTTTTTC-3'	5'-GCAGCATATTCCTGCGTAGATG-3'
<i>Ctsl</i>	5'-GTGGACTGTTCTCACGCTCA-3'	5'-TCCGTCCTTCGCTTCATAGG-3'
<i>Clcn1 +ex7a</i>	5'-GGGCGTGGGATGCTACTTTG-3'	5'-AGGACACGGAACACAAAGGC-3'
<i>Clcn1 pan</i>	5'-CTGACATCCTGACAGTGGGC-3'	5'-AGGACACGGAACACAAAGGC-3'
<i>Clcn1 (end-point)</i>	5'-GGAATACCTCACACTCAAGGCC-3'	5'-CACGGAACACAAAGGCACTGAATGT-3'
<i>Fbxo32</i>	5'-CTCTGTACCATGCCGTTCT-3'	5'-GGCTGCTGAACAGATTCTCC-3'
<i>GFP (multiplex)</i>	5'-ATAACTTGCTGGCCTTCCACT-3'	5'-CGGGCCATTTACCGTAAGTTAT-3'
		5'-GCAGCTCATTGCTGTTCTCAA-3'
<i>Insr +ex11</i>	5'-TATGACGACTCGGCCAGTGA-3'	5'-ACCATTGCCTGAAGAGGTTT-3'
<i>Insr pan</i>	5'-ATGGGCTTCGGGAGAGGAT-3'	5'-GGATGTCCATACCAGGGCAC-3'
<i>Map1lc3b</i>	5'-CACTGCTCTGTCTTGTGTAGGTTG-3'	5'-TCGTTGTGCCTTTATTAGTGCATC-3'
<i>Rbm3</i>	5'-CTTCTGCCATGTCGTCTGAA-3'	5'-TGGGTTTGTGAAGGTGATGA-3'
<i>Sqstm</i>	5'-GCTCAGGAGGAGACGATGAC-3'	5'-AGAAACCCATGGACAGCATC-3'
<i>Trim63</i>	5'-ACCTGCTGGTGGAAAACATC-3'	5'-AGGAGCAAGTAGGCACCTCA-3'

Supplemental Methods

Antibodies

The following antibodies were used for immunoblotting or immunofluorescence:

PKB/Akt (#9272), Phospho-Akt^{Ser473} (#4058), S6 (#2217), Phospho-S6^{Ser235/236} (#2211), Phospho-S6^{Ser240/244} (#2215), LC3B (#2775), AMPK α (#2532), Phospho-AMPK α ^{Thr172} (#2531), Ulk1 (#8054), Phospho-Ulk1^{Ser757} (#6888), Phospho-Ulk1^{Ser317} (#6887), mTOR (#2972), Phospho-mTOR^{Ser2448} (#2971), 4E-BP1 (#9452), Tuberin/TSC2 (#3635), Phospho-Tuberin/TSC2^{Ser1387} (#5584), Phospho-CaMKII^{Thr286} (#12716), LKB1 (#3047), TAK1 (#5206), p70S6K (#9202), Phospho-p70S6K^{Thr389} (#9209) from Cell Signaling; α -Actinin (A5044) from Sigma; p62 (GP62C) from Progen; α -Tubulin (ab15246), Laminin (ab11575 and ab11576), Lamp1 (AD4B) from Abcam; CaMKII (C-20) from Santa Cruz; MHCIIA (A4.74) and IIB (BF-F3) from DSHB. Clc-1 antibody was a generous gift from Prof. Thomas Cooper (Baylor College of Medicine, USA) (1). HRP-tagged and fluorescent secondary antibodies were from Abcam and Jackson ImmunoResearch. S6^{Ser235/236} blocking peptide was from Cell Signaling Technology (#1220).

Proteasome activity assay

Protein extracts and acquisition of proteasome activity using the Proteasome-Glo 3-Substrate System (Promega) was described before by Strucksberg et al.(2).

Transmission electronic microscopy (EM)

EM analysis was conducted on ultra-thin (70 nm) sections of gastrocnemius muscle, as previously described (3). Sections were stained with uranyl acetate and lead citrate, and observed on electron microscope (Philips CM100).

Supplemental References

1. Charlet BN, Savkur RS, Singh G, Philips AV, Grice EA, Cooper TA. Loss of the muscle-specific chloride channel in type 1 myotonic dystrophy due to misregulated alternative splicing. *Mol Cell*. 2002;10(1):45-53.
2. Strucksberg KH, Tangavelou K, Schroder R, Clemen CS. Proteasomal activity in skeletal muscle: a matter of assay design, muscle type, and age. *Anal Biochem*. 2010;399(2):225-229.
3. Moll J, Barzaghi P, Lin S, Bezakova G, Lochmuller H, Engvall E, Muller U, Ruegg MA. An agrin minigene rescues dystrophic symptoms in a mouse model for congenital muscular dystrophy. *Nature*. 2001;413(6853):302-307.